Supporting Information

Skau et al. 10.1073/pnas.1505035112

SI Materials and Methods

Cell Culture. Mice were maintained according to guidelines approved by the National Heart, Lung and Blood Institute Animal Care and Use Committee, NIH, Bethesda, MD. Embryonic day 13.5 (E13.5) embryos from C57J/BL6 × C57J/BL6 timed matings (mice obtained from The Jackson Laboratory) were dissected and decapitated and their internal organs removed. Tissue was cut into pieces and incubated at 37 °C for 30 min in 0.25 mg/mL Trypsin-EDTA (Life Technologies) with mild vortexing every 10 min. After digestion, cell suspension was passed through a 100-μm nylon-mesh cell strainer and then cells were precipitated by centrifugation for 8 min. Media containing trypsin, lipids, etc. were removed and single mouse embryonic fibroblasts (MEFs) were resuspended and transferred to sterile tissue culture dishes in DMEM/20% (vol/vol) FBS (Gibco). Nonadherent cells were removed after 4 h. Adherent cells were allowed to attach overnight then subcultured for transfection or frozen in liquid nitrogen in FBS/10% (vol/vol) DMSO without further passaging. Human foreskin fibroblasts were obtained from ATCC and maintained at 37 °C in DMEM/10% (vol/vol) FBS at 5% CO_2/95% (vol/vol) air. MEFs were maintained in DMEM/20% FBS and passaged no more than six times.

Reagents and Transfection. cDNA encoding mApple- or EGFP-actin, EGFP-, mCherry-, or mApple-paxillin were a gift from M. Davidson, Florida State University, Tallahassee, FL. INF2-GFP was a gift from H. Higgs, Dartmouth University, Hanover, NH. MEFs were transiently transfected using Amaxa Kit V solution (Amaxa Nucleofector, Lonza), program "MEF alternate program A-023," and 1 μg DNA was then recovered in DMEM/20% (vol/vol) FBS overnight before plating on coverslips coated with 5 μg/mL human plasma fibronectin for all constructs except the INF2-GFP rescue construct, which was recovered in DMEM/20% (vol/vol) FBS for 3–4 h on glass coverslips coated with 5 μg/mL (wt/vol) human plasma fibronectin and then imaged immediately (see below for imaging conditions). ON-TARGETplus SMARTpool siRNA against INF2 was purchased from GE Healthcare Dharmacon. The myosin II inhibitor blebbistatin was purchased from Toronto Research Chemicals and used at 50 μM for 2 h. Alexa-488 phalloidin was obtained from Invitrogen. Rhodamine-labeled rabbit muscle G-actin was purchased from Cytoskeleton (catalog no. AR05), resuspended as described in the manufacturer's protocol, and stored at 4 °C. Immediately before use, 10 μL was centrifuged at 100,000 × *g* for 30 min in a Sorvall RC M120 GX centrifuge, S55-S swinging bucket rotor, and only the top 7 μL was used. Alexa-647–labeled fibronectin was a gift from K. Yamada, NIH, Bethesda, and was used at 2.5 μg/mL with 2.5 μg/mL unlabeled human plasma fibronectin added simultaneously.

The following primary antibodies were used for indirect immunofluorescence: anti-INF2 (rabbit; ProteinTech) antipaxillin clone 349, anti-FAK clone 77 (both mouse; BD Biosciences); antiphosphopaxillin (rabbit catalog no. 44–720G; Life Technologies); antiphospho-FAK clone 31H5L17 (rabbit; Invitrogen/Life Technologies); antitensin (rabbit; gift from B Geiger, Weizmann Institute of Science, Rehovot, Israel); anti-VASP clone 9A2, antimyosin-IIA catalog no. 3403P; and antiphosphomyosin-light-chain II T18/S19 catalog no. 3674P (all rabbit; Cell Signaling Technologies); anti–α-actinin clone BM-75.2, antitropomyosin clone TM311, antitalin clone 8D4, antivinculin clone VIN-11–5; (all mouse; Sigma-Aldrich); antivinculin (rabbit, catalog no. V4139; Sigma-Aldrich); antiphosphotyrosine clone 4G10, anti-GFP chicken catalog no. 06–896 (EMD Millipore); anti-GFP (rabbit catalog no. ab290; Abcam); antizyxin (rabbit; gift from M. Beckerle, University of Utah, Salt Lake City); and anti-myosin-IIB (rabbit catalog no. PRB-445P; BioLegend/Covance). The following secondary antibodies were used for indirect immunofluorescence: donkey anti-rabbit Alexa 647 conjugate, donkey anti-mouse Cy3 conjugate, and anti-chicken Cy3 conjugate (Jackson ImmunoResearch Laboratories).

Fixation and Immunofluorescence. For staining of endogenous INF2, cells were fixed with ice-cold acetone. Cells plated on glass coverslips coated with 5 μg/mL human plasma fibronectin (EMD Millipore) were rinsed twice with warm 1× PBS. Coverslips were removed from PBS and immediately immersed in −20 °C acetone and incubated at −20 °C in acetone for 10 min. Coverslips were removed from acetone and rinsed with 1× cytoskeleton buffer (10 mM Mes pH 6.1, 138 mM KCL, 3 mM $MgCl_2$, 2 mM EGTA) for 10 min and then washed three times with 1× TBS. Fixed coverslips were then incubated for at least 1 h in 2% (wt/vol) BSA in cytoskeleton buffer with Alexa-488 phalloidin (1:400 dilution) and then for at least 2 h in primary antibody diluted in 2% (wt/vol) BSA in TBS (anti-INF2 was used at 1:150, other antibodies at 1:200). After washing three times with 1× TBS, coverslips were incubated at least 1 h in fluorescently conjugated secondary antibody (1:250 dilution anti-rabbit Alexa-647 and anti-mouse Cy3). Coverslips were washed three times with 1× TBS and then mounted on glass slides with DAKO fluorescent mounting medium.

For fixation of mock-transfected and INF2 KD MEFs, indirect immunofluorescence was performed as described (1). Briefly, cells plated on 5 μg/mL fibronectin overnight were fixed for 20 min with 4% (vol/vol) paraformaldehyde in cytoskeleton buffer (Electron Microscopy Science), permeabilized with 0.5% Triton X-100 in cytoskeleton buffer, and then washed with 0.1 M glycine (vol/vol) in cytoskeleton buffer followed by three washes with 1× TBS. Fixed cells were blocked for at least 1 h in 2% (wt/vol) BSA/0.1% Tween-20 with Alexa-488 phalloidin (1:400 dilution, Invitrogen) in TBS and incubated for at least 2 h in primary antibody, washed, and incubated at least 1 h in fluorescently conjugated secondary antibody. Coverslips were then mounted on glass slides with DAKO fluorescent mounting media (Agilent Technologies).

For the detection of free barbed ends, cells plated on 5 μg/mL fibronectin overnight were rinsed with rinse buffer (138 mM KCl, 20 mM Hepes pH 7.5, 4 mM $MgCl_2$, 3 mM EGTA). Rhodamine-labeled G-actin (Cytoskeleton) was diluted to a final concentration of 0.5 μM in rinse buffer + 0.025% saponin + 0.1 mM DTT + 2 mM ATP. Diluted actin was slowly added to the top surface of the coverslip and incubated for 2 min and 15 s and then wicked off. Coverslips were incubated in 1× cytoskeleton buffer + 0.5% glutaraldehyde for 10 min and then 1× cytoskeleton buffer + 0.2% Triton X-100 for 30 s. Coverslips were quenched with 0.5 mg/mL $NaBH_4$ in PBS for 10 min. Fixed cells were then blocked and stained as described above for paraformaldehyde fixation/staining, using a 1:250 dilution of mouse antipaxillin (clone 349; BD Biosciences) as the focal adhesion marker.

Imaging. Spinning disk confocal imaging of both fixed and live cells was performed with a Plan Apo 60× 1.40 NA Ph oil immersion objective lens on an inverted Eclipse Ti microscope system (Nikon Instruments) equipped with the Nikon PerfectFocus system, a servo-motor controlled X–Y stage and a PZ-2000 Piezo

Z stage (Applied Scientific Instrumentation), and a spinning disk confocal scan head (CSU-X; Yokogawa). Laser illumination was provided by 488 nm, 561 nm, and/or 655 nm solid state lasers fitted in a custom laser combiner module (Spectral Applied Research) and delivered to the confocal scan head or the Nikon TIRF illuminator via a single mode optical fiber (Oz Optics). Photobleaching was accomplished using a FRAPPA dual galvanometer scan head (Andor Technology). An appropriate multibandpass dichromatic mirror and single bandpass emission filters (Semrock Technologies) were used to select emission wavelength. Pairs or sets of three images were captured in immediate succession with one of two cooled CCD cameras (CoolSNAP HQ2 or CoolSNAP MYO; Photometrics) operated in the 14-bit mode. For live cell imaging, temperature was controlled with either an Air Stream Stage Incubator (Nevtek) or a LiveCell Incubation Chamber (Pathology Devices) which also controlled humidity. Dual-color time-lapse TIRF microscopy of EGFP and mApple- or mCherry-tagged proteins in living cells was performed at 37 °C using an Apo TIRF 100 × 1.49 NA oil immersion objective lens (Nikon Instruments) on an inverted Eclipse Ti microscope system (Nikon Instruments) with an evanescent field depth of ∼150 nm. Pairs of EGFP (using 488 nm laser illumination) and mCherry or mApple (using 561 nm laser illumination) images were captured in rapid succession at 5-s intervals using either an EMCCD camera (Cascade II:1024; Photometrics) or cooled CCD (CoolSNAP HQ2, Photometrics). Long-term phase-contrast imaging of individual cells migrating randomly on coverslips coated with 5 μg/mL human plasma fibronectin was performed on an inverted Eclipse Ti microscope system (Nikon Instruments) with a Plan Fluor 10×/0.30 NA dry objective lens (Nikon Instruments). Pairs of phase contrast and EGFP spinning-disk confocal (using 488 nm laser illumination) images were captured at 5-min intervals at multiple stage positions for 16 h. All live cell experiments were performed in Phenol red–free DMEM containing 5% (vol/vol) FBS, 20 mM Hepes, and 10 units/mL oxyrase (Oxyrase) as imaging medium. All electronic functions on the Eclipse Ti microscope systems were controlled by MetaMorph imaging software (Molecular Devices).

Image Analysis. For colocalization analysis, Pearson's coefficient was determined using the JACoP plugin for ImageJ (NIH) as described previously (2). Lamellipodia width, fraction of cell perimeter that is lamellipodium, and number and length of stress fibers were determined by hand tracing the relevant features on Alexa-488 phalloidin-stained images of control and INF2 KD MEFs. Cell size was determined by hand tracing the outline of cells based on Alexa-488 phalloidin stained images. G-actin incorporation was determined by outlining FAs based on paxillin immunofluorescence or lamellipodia based on Alexa-488 phalloidin staining, then measuring rhodamine fluorescence at FA or lamellipodium, subtracting background and normalizing for adhesion or lamellipodial size. Adhesion size and aspect ratio were measured by hand tracing adhesions on paxillin immunofluorescence images. Adhesion lifetime was measured from TIRF image sequences taken every 5 s of EGFP-paxillin in control and INF2 KD cells. Nucleation rate was measured by overlaying two TIRF images of EGFP-paxillin taken 100 s apart and counting newly generated adhesions and then tiling this procedure every 10 s for 20 min. Random cell migration analysis (velocity, directionality, and trajectory plots) was performed using the Chemotaxis and Migration Tool 2.0 (Ibidi) on 15 cells for each condition.

Traction force microscopy (TFM) was performed as described previously (3–5). Briefly, cells transfected with EGFP-paxillin were plated on polyacrylamide gels of stiffness, 8.6 kPa, embedded with 568 and 655 fluorescent microspheres and images acquired before and after release of cells with trypsin. Images of deformed and relaxed substrates were aligned and movement of microspheres was quantified with subpixel accuracy using custom-generated MatLab software (3–5).

Generation of Cell-Derived Matrices. Cell-derived matrices were produced as previously described (6) using human foreskin fibroblasts (ATCC) maintained in DMEM/15% (vol/vol) FBS and transfected with Amaxa solution NHDF, program "NHDF, human, neonatal U-020" with 2 μg of shRNA (pGIPZ system; Open Biosystems/GE Healthcare) and plated to confluency on MatTek dishes treated with glutaraldhyde-crosslinked gelatin and coated with 10 μg/mL human plasma fibronectin. After 24 h, media was exchanged for DMEM/15% (vol/vol) FBS with 100 μg/mL ascorbic acid. Confluent cultures were maintained at 37 °C with 5% CO_2/95% (vol/vol) air for 5–7 d with media exchanged every 48 h for new DMEM/15% FBS with 100 μg/mL ascorbic acid; every 24 h GFP fluorescence was monitored to determine maintenance of shRNA. After 5–7 d when GFP fluorescence began to decline, matrices were washed once with warm 1× PBS and then incubated for 5 min with cell lysis buffer [0.5% (vol/vol) Triton X-100, 20 mM NH_4OH in sterile 1× PBS] and monitored for lysis by low-magnification microscopy (EVOS FL Cell Imaging System; Life Technologies). After complete cell lysis, matrices were washed twice with warm 1× PBS and then incubated in 1× PBS overnight at 4 °C. After incubation, matrices were washed once with 1× PBS and then incubated with 20 units DNase I (Roche). DNase I was removed, matrices were washed once with 1× PBS, and matrices were imaged at 4× magnification using phase contrast optics on the EVOS FL Cell Imaging System.

1. Pasapera AM, Schneider IC, Rericha E, Schlaepfer DD, Waterman CM (2010) Myosin II activity regulates vinculin recruitment to focal adhesions through FAK-mediated paxillin phosphorylation. *J Cell Biol* 188(6):877–890.
2. Bolte S, Cordelières FP (2006) A guided tour into subcellular colocalization analysis in light microscopy. *J Microsc* 224(Pt 3):213–232.
3. Gardel ML, et al. (2008) Traction stress in focal adhesions correlates biphasically with actin retrograde flow speed. *J Cell Biol* 183(6):999–1005.
4. Plotnikov SV, Sabass B, Schwarz US, Waterman CM (2014) High-resolution traction force microscopy. *Methods Cell Biol* 123:367–394.
5. Sabass B, Gardel ML, Waterman CM, Schwarz US (2008) High resolution traction force microscopy based on experimental and computational advances. *Biophys J* 94(1): 207–220.
6. Kutys ML, Doyle AD, Yamada KM (2013) Regulation of cell adhesion and migration by cell-derived matrices. *Exp Cell Res* 319(16):2434–2439.

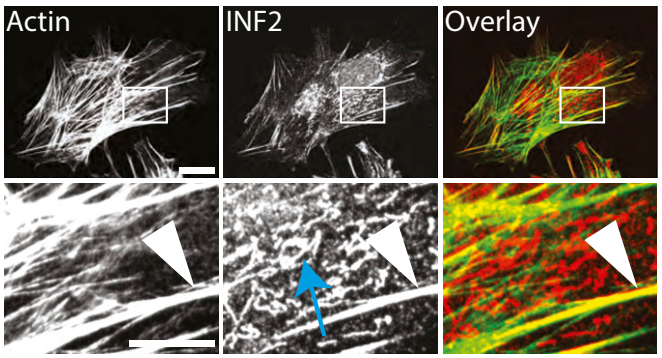

Fig. S1. Endogenous INF2 localizes to mitochondria-like structures in the center of the cell. Representative spinning disk confocal micrographs of MEF with Alexa-488 phalloidin staining of actin (green) with immunofluorescence of INF2 (red). White arrowheads indicate colocalization of INF2 and actin at stress fibers. Blue arrow indicates localization of INF2 but not actin to narrow fibril structures presumed to be mitochondria in the center of the cell. [Scale bar, (*Top*) 20 μm; (*Bottom*) 10 μm.]

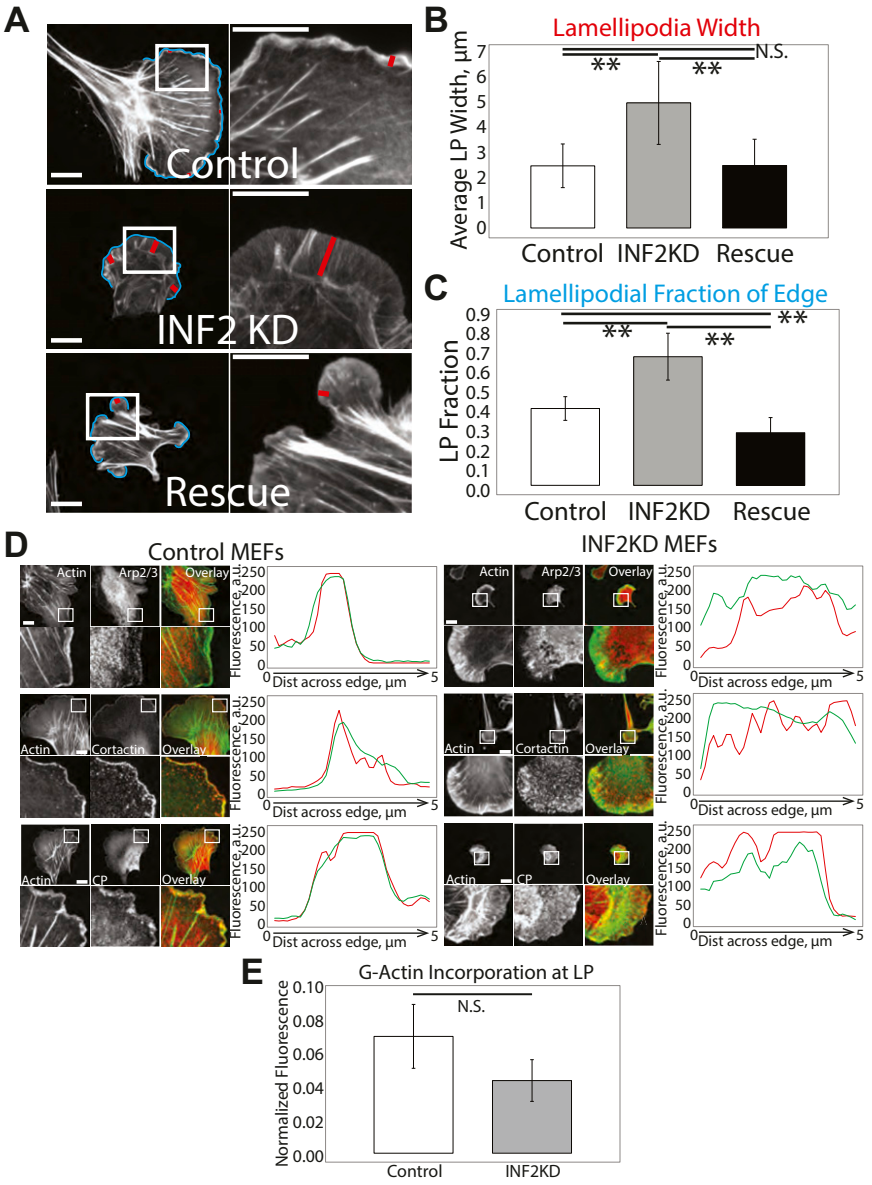

Fig. S2. INF2 limits the width of the lamellipodium. (*A*) Representative confocal micrographs of Alexa-488 phalloidin staining of actin in mock-transfected (control), MEFs transfected with siRNA targeting INF2 (INF2 KD), and INF2 KD MEFs reexpressing the human INF2 isoform lacking the mitochondrial targeting sequence fused to GFP (rescue). Blue line highlights the part of the cell perimeter that is counted as lamellipodium. Red bars indicate width of lamellipodia. White boxes indicate area zoomed at *Right*. [Scale bar, (*Left*) 10 µm; (*Right*) 5 µm.] (*B* and *C*) Bar graphs of lamellipodial characteristics. (*B*) The average width of lamellipodia and (*C*) the fraction of the cell perimeter that is lamellipodium. $n = 10$ cells per condition. Error bar: SD. $^{**}P < 0.01$, N.S., not significant, Student's *t* test. (*D*, *Left*) Alexa-488 phalloidin staining of actin (green) and immunofluorescence of lamellipodia proteins in mock transfected (control) and MEFs transfected with siRNA targeting INF2 (INF2 KD). (*Top*) The Arp2/3 complex, (*Middle*) cortactin, (*Bottom*) capping protein (CP), all in red. White boxes indicate area zoomed below. (Scale bar, 10 µm.) (*Right*) Graphs of line scans of fluorescence intensities across the leading edge of control and INF2 KD MEFs. Green traces are Alexa-488 phalloidin staining of actin; red traces are immunofluorescence of lamellipodia proteins. (*E*, *Right*) Bar graph of normalized G-actin incorporation at FAs as measured by the ratio of X-rhodamine G-actin fluorescence to Alexa-488 phalloidin fluorescence in lamellipodia (LP). $n = 5$ cells per condition. N.S., not significant, Student's *t* test.

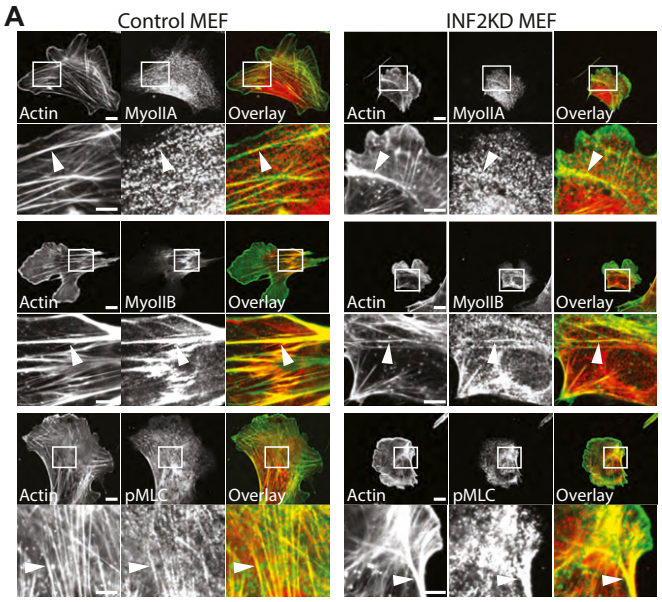

Fig. S3. INF2 is not critical for ventral SFs or rear actin bundles. Representative spinning disk confocal micrographs of mock-transfected (control, *Left*) and MEFs transfected with siRNAs targeting INF2 (INF2 KD, *Right*). (*A*) Alexa-488 phalloidin staining of actin (green) and immunofluorescence of myosin II. (*Top*) Myosin IIA isoform; (*Middle*) myosin IIB isoform; (*Bottom*) phosphorylated (T18/S19) myosin II regulatory light chain, all in red. White boxes indicate area zoomed below. White arrowheads indicate decoration of actin fibers by myosin. [Scale bar, (*Top*) 10 μm; (*Bottom*) 5 μm.]

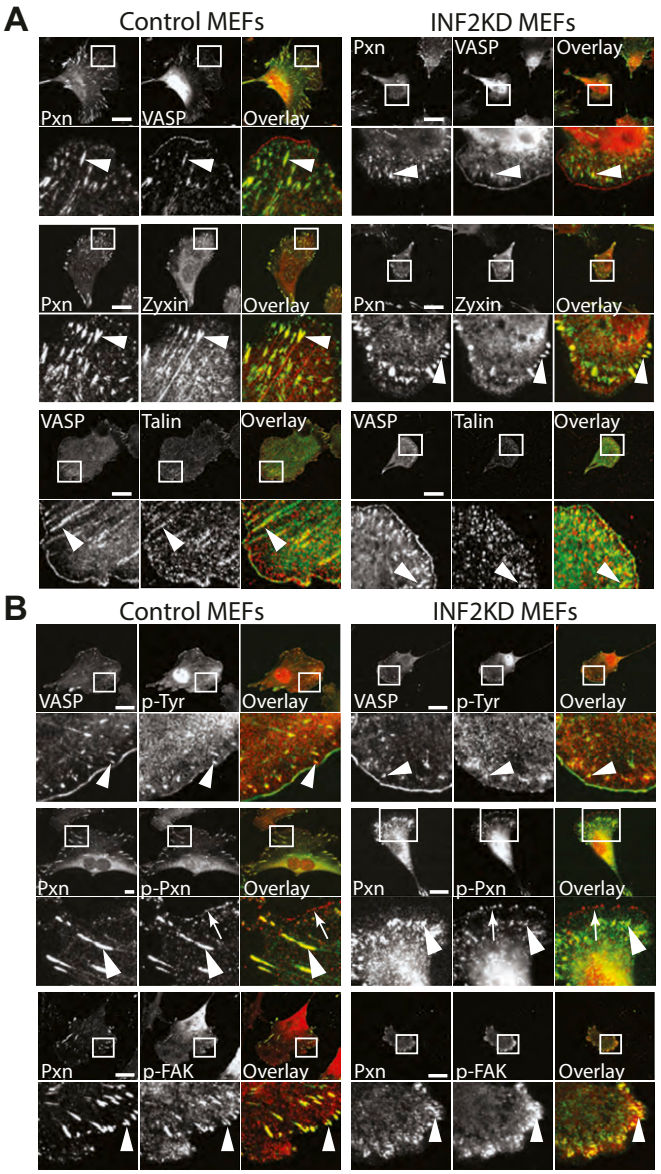

Fig. S4. INF2 is not essential for localization of many canonical FA proteins. (*A*) Representative confocal micrographs of coimmunofluorescence of pairs of known FA proteins [paxillin (Pxn), VASP, zyxin, and talin] in mock-transfected (control, *Left*) and MEFs transfected with siRNAs targeting INF2 (INF2 KD; *Right*). White boxes indicate area zoomed below. White arrowheads indicate colocalization of proteins at FAs. (Scale bar, 10 μm.) (*B*) Representative confocal micrographs of coimmunofluorescence of FA proteins (paxillin or VASP, green) with phospho-specific antibodies against FA signaling molecules (red) in control and INF2 KD MEFs: Total phosphotyrosine (p-Tyr), paxillin phosphorylated on tyrosine 31 (p-Pxn), and FAK phosphorylated on tyrosine 297 (p-FAK). White boxes indicate area zoomed below. White arrowheads indicate colocalization of proteins at FA. (Scale bar, 10 μm.)

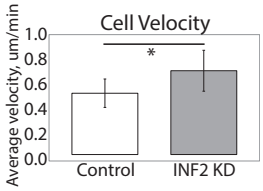

Fig. S5. INF2 does not directly drive cell migration velocity. Bar graph of average velocity of mock-transfected (control) and MEFs transfected with siRNA targeting INF2 (INF2 KD) randomly migrating on fibronectin-coated glass. $n = 15$ cells per condition. Error bar: SD. $^*P < 0.05$, Student's t test.

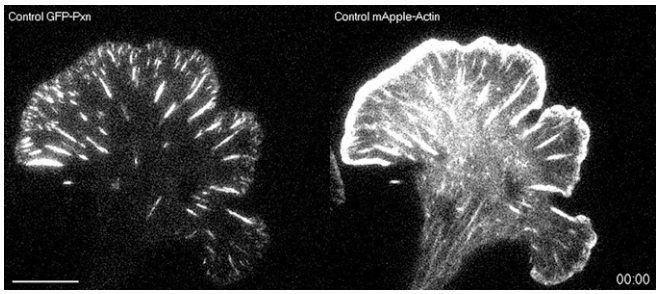

Movie S1. Dynamics of paxillin at focal adhesions and actin at stress fibers in MEF. MEF expressing paxillin-EGFP (*Left*) and mApple-Actin (*Right*) were cultured on fibronectin-coated coverslips and imaged by TIRF microscopy. Time indicates minutes:seconds. (Scale bar, 10 μm.)

Movie S1

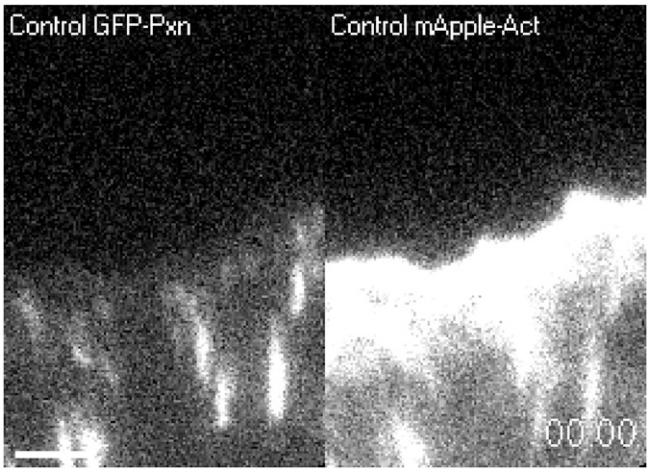

Movie S2. High magnification of paxillin and actin at the leading edge of MEF. Zoom of cell edge of MEF expressing paxillin-EGFP (*Left*) and mApple-Actin (*Right*) that were cultured on fibronectin-coated coverslips and imaged by TIRF microscopy. Time indicates minutes:seconds. (Scale bar, 2 μm.)

Movie S2

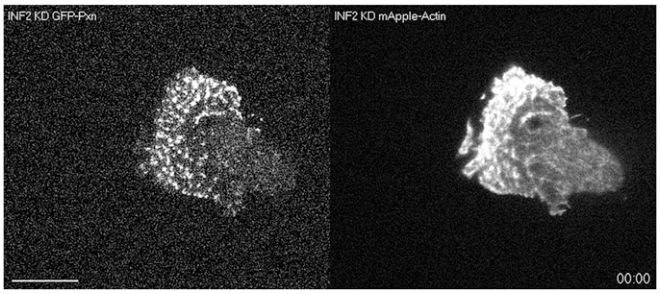

Movie S3. Dynamics of paxillin at focal adhesions and actin at stress fibers in INF2 KD MEF. MEF transfected with siRNA targeting INF2 (INF2 KD) expressing paxillin-EGFP (*Left*) and mApple-Actin (*Right*) were cultured on fibronectin-coated coverslips and imaged by TIRF microscopy. Time indicates minutes:seconds. (Scale bar, 10 μm.)

Movie S3

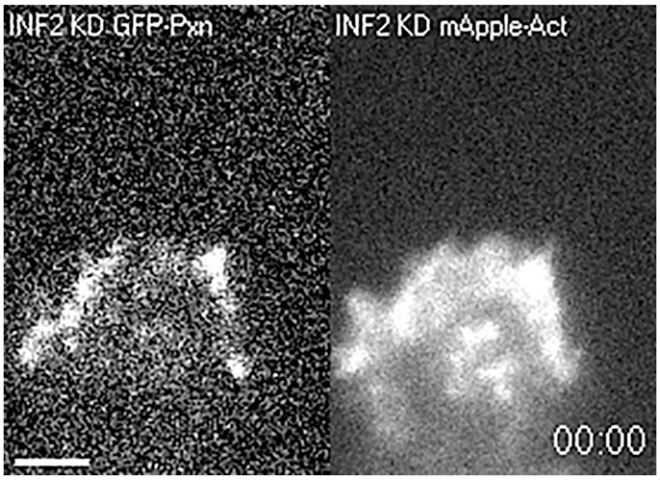

Movie S4. High magnification of paxillin and actin at the leading edge of INF2 KD MEF. Zoom of cell edge of MEF transfected with siRNA targeting INF2 (INF2 KD) expressing paxillin-EGFP (*Left*) and mApple-Actin (*Right*) that were cultured on fibronectin-coated coverslips and imaged by TIRF microscopy. Time indicates minutes:seconds. (Scale bar, 2 μm.)

Movie S4

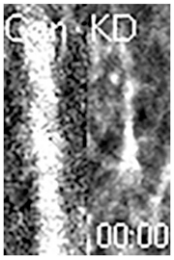

Movie S5. Comparison of dorsal SF elongation in control and INF2 KD MEF. Individual dorsal SF in mock transfected MEF (Con, *Left*) or MEF transfected with siRNA targeting INF2 (KD, *Right*) cultured on fibronectin-coated coverslips expressing mApple-Actin were photobleached and imaged by spinning disk confocal microscopy. Time indicates minutes:seconds. (Scale bar, 10 μm.)

Movie S5

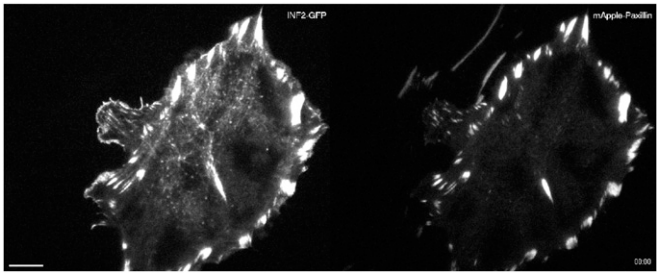

Movie S6. Dynamics of INF2-GFP and mApple-paxillin at focal adhesions and the leading edge of MEF. MEF expressing human INF2-GFP lacking the membrane-targeting CAAX domain (*Left*) and mApple-paxillin (*Right*) were cultured on fibronectin-coated coverslips and imaged by TIRF microscopy. Time indicates minutes:seconds. (Scale bar, 10 μm.)

Movie S6

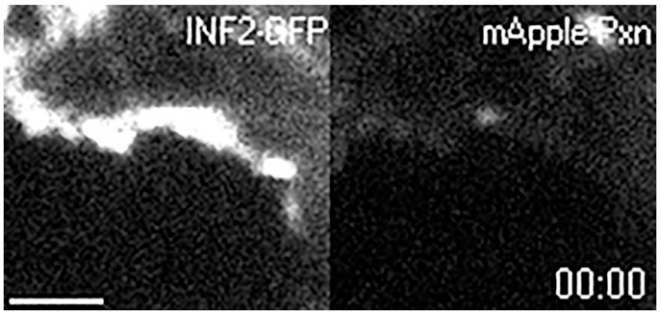

Movie S7. High magnification of INF2-GFP and mApple-paxillin dynamics at the leading edge of MEF. Zoom of protruding cell edge of MEF expressing human INF2-GFP lacking the membrane-targeting CAAX domain (*Left*) and mApple-paxillin (*Right*) were cultured on fibronectin-coated coverslips and imaged by TIRF microscopy. Time indicates minutes:seconds. (Scale bar, 1 μm.)

Movie S7

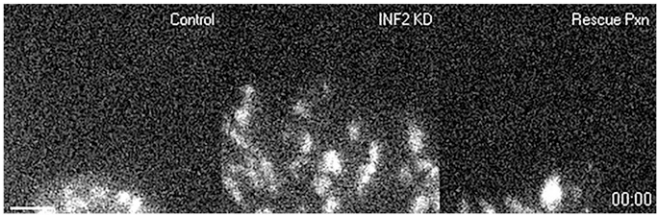

Movie S8. Dynamics of focal adhesion assembly in control, INF2 KD, and rescue MEF. Mock-transfected MEF (control, *Left*), MEF transfected with siRNA targeting INF2 (INF2 KD, *Center*) and INF2 KD cells reexpressing the human INF2-GFP isoform lacking the mitochondrial targeting sequence (rescue, *Right*) expressing paxillin-EGFP were cultured on fibronectin-coated coverslips and imaged by TIRF microscopy. Time indicates minutes:seconds. (Scale bar, 2 μm.)

Movie S8

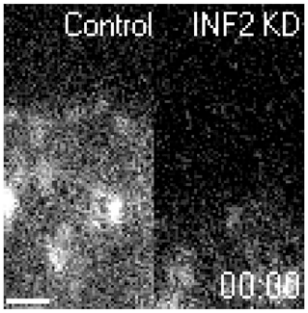

Movie S9. Dynamics of focal adhesion assembly in control, INF2 KD. Mock-transfected MEF (control, *Left*) or MEF transfected with siRNA targeting INF2 (INF2 KD, *Right*) expressing paxillin-EGFP were cultured on fibronectin-coated coverslips and imaged by TIRF microscopy. Time indicates minutes:seconds. (Scale bar, 2 μm.)

Movie S9